

Fundamental limits on the rate of bacterial cell division

Nathan M. Belliveau^{†, 1}, Griffin Chure^{†, 2, 3}, Christina L. Hueschen⁴, Hernan G. Garcia⁵, Jané Kondev⁶, Daniel S. Fisher⁷, Julie Theriot^{1, 8}, Rob Phillips^{2, 9,*}

*For correspondence:

[†]These authors contributed equally to this work

¹Department of Biology, University of Washington, Seattle, WA, USA; ²Division of Biology and Biological Engineering, California Institute of Technology, Pasadena, CA, USA; ³Department of Applied Physics, California Institute of Technology, Pasadena, CA, USA; ⁴Department of Chemical Engineering, Stanford University, Stanford, CA, USA; ⁵Department of Molecular Cell Biology and Department of Physics, University of California Berkeley, Berkeley, CA, USA; ⁶Department of Physics, Brandeis University, Waltham, MA, USA; ⁷Department of Applied Physics, Stanford University, Stanford, CA, USA; ⁸Allen Institute for Cell Science, Seattle, WA, USA; ⁹Department of Physics, California Institute of Technology, Pasadena, CA, USA; *Contributed equally

14

Abstract This will be written next

16

Translation and ribosomal synthesis

Lastly, we turn our attention to the process of translation. [expand on.]

tRNA synthetases

[expand on]

We begin by first estimating the number of tRNA synthetases. *E. coli* has roughly 3×10^6 proteins per cell, which for an average protein of 300 aa, amounts to the formation of $\approx 10^9$ peptide bonds. This value will also match the number of amino-acyl tRNA that are required for protein synthesis, with the pool of tRNA continuously recharging new amino acids by tRNA synthetases. At a rate of charging of about 20 amino-acyl tRNA per second (BNID: 105279, *Milo et al. (2010)*), we find that cells have more than sufficient tRNA synthetases to meet the ribosomal demand (*Figure 1(A)*).

Protein synthesis

[expand on]

If we consider an elongation rate of ≈ 15 peptide bonds per second (BNID: 114271, *Milo et al. (2010); Dai et al. (2016)*), the formation of $\approx 10^9$ peptide bonds would require about 1.5×10^4 ribosomes. This is indeed consistent with the experimental data shown in *Figure 1(B)*.

Ribosomal synthesis

So far our estimates have led to protein copy numbers that are consistent with the proteomic data, or even in excess of what might be needed for each task under limiting growth conditions. Even in our example of *E. coli* grown under different carbohydrate sources (??(B)), it becomes clear cells can utilize alternative carbon sources by inducing the expression of additional membrane transporters and enzymes. Optimal resource allocation and the role of ribosomal proteins have been an area of intense quantitative study over the last decade by Hwa and others (*Scott et al., 2010; Hui et al., 2015*). From the perspective of limiting growth, our earlier estimate of rRNA

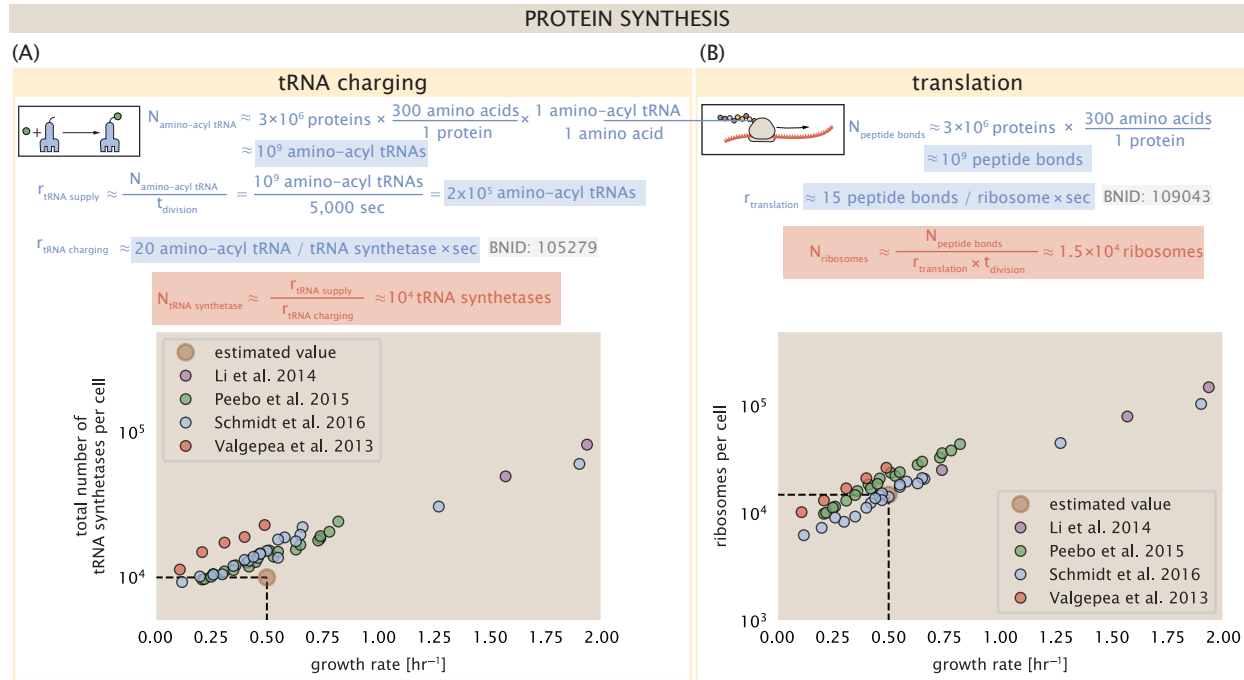


Figure 1. Estimation of the required tRNA synthetases and ribosomes. (A) Estimation for the number of tRNA synthetases that will supply the required amino acid demand. The sum of all tRNA synthetases copy numbers are plotted as a function of growth rate ([ArgS], [CysS], [GlnS], [GltX], [IleS], [LeuS], [ValS], [AlaS]₂, [AsnS]₂, [AspS]₂, [TyrS]₂, [TrpS]₂, [ThrS]₂, [SerS]₂, [ProS]₂, [PheS]₂[PheT]₂, [MetG]₂, [lysS]₂, [HisS]₂, [GlyS]₂[GlyQ]₂). (B) Estimation of the number of ribosomes required to synthesize 10⁹ peptide bonds with an elongation rate of 15 peptide bonds per second. The average abundance of ribosomes is plotted as a function of growth rate. Our estimated values are shown for a growth rate of 0.5 hr⁻¹.

40 highlighted the necessity for multiple copies of rRNA genes in order to make enough rRNA. For
 41 *E. coli*'s fastest growth rates at 2 hr⁻¹, the additional demand for rRNA is further supported by
 42 parallelized DNA replication and increased rRNA gene dosage. This suggests the possibility that
 43 synthesis of ribosomes might be rate limiting. While the transcriptional demand for the ribosomal
 44 proteins is substantially lower than rRNA genes, since proteins can be translated from relatively
 45 fewer mRNA, other ribosomal proteins like the translation elongation factor EF-Tu also present a
 46 substantial burden. For EF-Tu in particular, it is the most highly expressed protein in *E. coli* and is
 47 expressed from multiple gene copies, *tufA* and *tufB*.

48 To gain some intuition into how translation may set the speed limit for bacterial growth, we
 49 again consider the total number of peptide bonds that must be synthesized, N_{AA} . Noting that cell
 50 mass grows exponentially (**Godin et al., 2010**), we can compute the number of amino acids to be
 51 polymerized as

$$N_{\text{AA}} = \frac{r_t R}{\lambda}, \quad (1)$$

52 where λ is the cell growth rate in s⁻¹, r_t is the maximum translation rate in amino acids per second,
 53 and R is the average ribosome copy number per cell. Knowing the number of peptide bonds to be
 54 formed permits us to compute the translation-limited growth rate as

$$\lambda_{\text{translation-limited}} = \frac{r_t R}{N_{\text{AA}}}. \quad (2)$$

55 Alternatively, since N_{AA} is related to the total protein mass through the molecular weight of
 56 each protein, we can also consider the growth rate in terms of the fraction of the total proteome
 57 mass that is dedicated to ribosomal protein mass. By making the approximation that an average
 58 amino acid has a molecular weight of 110 Da (see **Figure 2(A)**), we can rewrite the growth rate as,

$$\lambda_{\text{translation-limited}} \approx \frac{r_t}{L_R} \Phi_R, \quad (3)$$

59 where L_R is the total length in amino acids that make up a ribosome, and Φ_R is the ribosomal mass
 60 fraction. This is plotted as a function of ribosomal fraction Φ_R in **Figure 2(A)**, where we take $L_R \approx$
 61 7500 aa, corresponding to the length in amino acids for all ribosomal subunits of the 50S and 30S
 62 complex (BNID: 101175, (*Milo et al., 2010*)). This formulation assumes that the cell can transcribe
 63 the required amount of rRNA, which appears reasonable for *E. coli*, allowing us to consider the
 64 inherent limit on growth set by the ribosome.

65 The growth rate defined by Equation 3 reflects mass-balance under steady-state growth and
 66 has long provided a rationalization to the apparent linear increase in *E. coli*'s ribosomal content
 67 as a function of growth rate (*Maaløe, 1979; Scott et al., 2010*). For our purposes, there are several
 68 important consequences of this trend. Firstly, we note there is a maximum growth rate of $\lambda \approx 6\text{hr}^{-1}$,
 69 or doubling time of about 7 minutes (dashed line). This growth rate can be viewed as an inherent
 70 maximum growth rate due to the need for the cell to double the cell's entire ribosomal mass.
 71 Interestingly, this limit is independent of the absolute number of ribosomes and is simply given
 72 by time to translate an entire ribosome, L_R/r_i . As shown in **Figure 2(B)**, we can reconcile this with
 73 the observation that in order to double the average number of ribosomes, each ribosome must
 74 produce a second ribosome. Unlike DNA replication or rRNA transcription, this is a process that
 75 cannot be parallelized.

76 For reasonable values of Φ_R , between about 0.1 - 0.3 (*Scott et al., 2010*), the maximum growth
 77 rate is in line with experimentally reported growth rates around 0.5 - 2 hr^{-1} . Importantly, in
 78 order for a cell to scale this growth limit they *must* increase their ribosomal abundance. This can
 79 be achieved by either synthesizing more ribosomes or reducing the fraction of non-ribosomal
 80 proteins. Reduction of non-ribosomal proteins is not a straightforward task since (as we have
 81 found throughout our estimates) doubling a cell requires many other enzymes and transporters.
 82 Increasing the absolute ribosomal abundance in *E. coli* will be limited by the number of rRNA
 83 operons.

84 Here we again return to rRNA synthesis, but here consider the maximum rRNA that can be
 85 produced at different growth rates.

86 [expand on.]

87 Discussion

88 [Fill in.]

89 Maximizing growth rate requires coordination of biosynthesis at all growth rates.

90 However, the mechanism behind growth rate control has remained elusive and has only been
 91 described at a phenomenological level.

92 Here we attempt to place our observations across the proteomic data sets in the context of *E.*
coli maximizing its steady-state growth rate across a wide array of conditions.

94 Parallel DNA replication biases gene dosage in support of ribosome synthesis.

95 *E. coli* cells grow by a so-called "adder" mechanism, whereby cells add a constant volume with
 96 each cell division (*Taheri-Araghi et al., 2015*). In conjunction with this, additional rounds of DNA
 97 replication are triggered when cells reach a critical volume per origin of replication (**Figure 3(A)**).
 98 This leads to the classically-described exponential increase in cell size with growth rate *Schaechter*
 99 *et al. (1958); Si et al. (2017, 2019)*. In the context of maximizing growth rate, it is notable that the
 100 majority of ribosomal proteins and rRNA operons are found closer to the DNA origin.

101 While an increase in transcription has been observed for genes closer to the origin in rapidly
 102 growing *E. coli* (*Scholz et al., 2019*), we were unaware of such characterization at the proteomic
 103 level. In order to see whether there is a relative increase in protein expression for genes closer to
 104 the origin at faster growth, we calculated a running boxcar average (500 kbp window) of protein
 105 copy number as a function of each gene's transcriptional start site (**Figure 3(B)**). While absolute
 106 protein copy numbers can vary substantially across the chromosome, we indeed observe a bias in

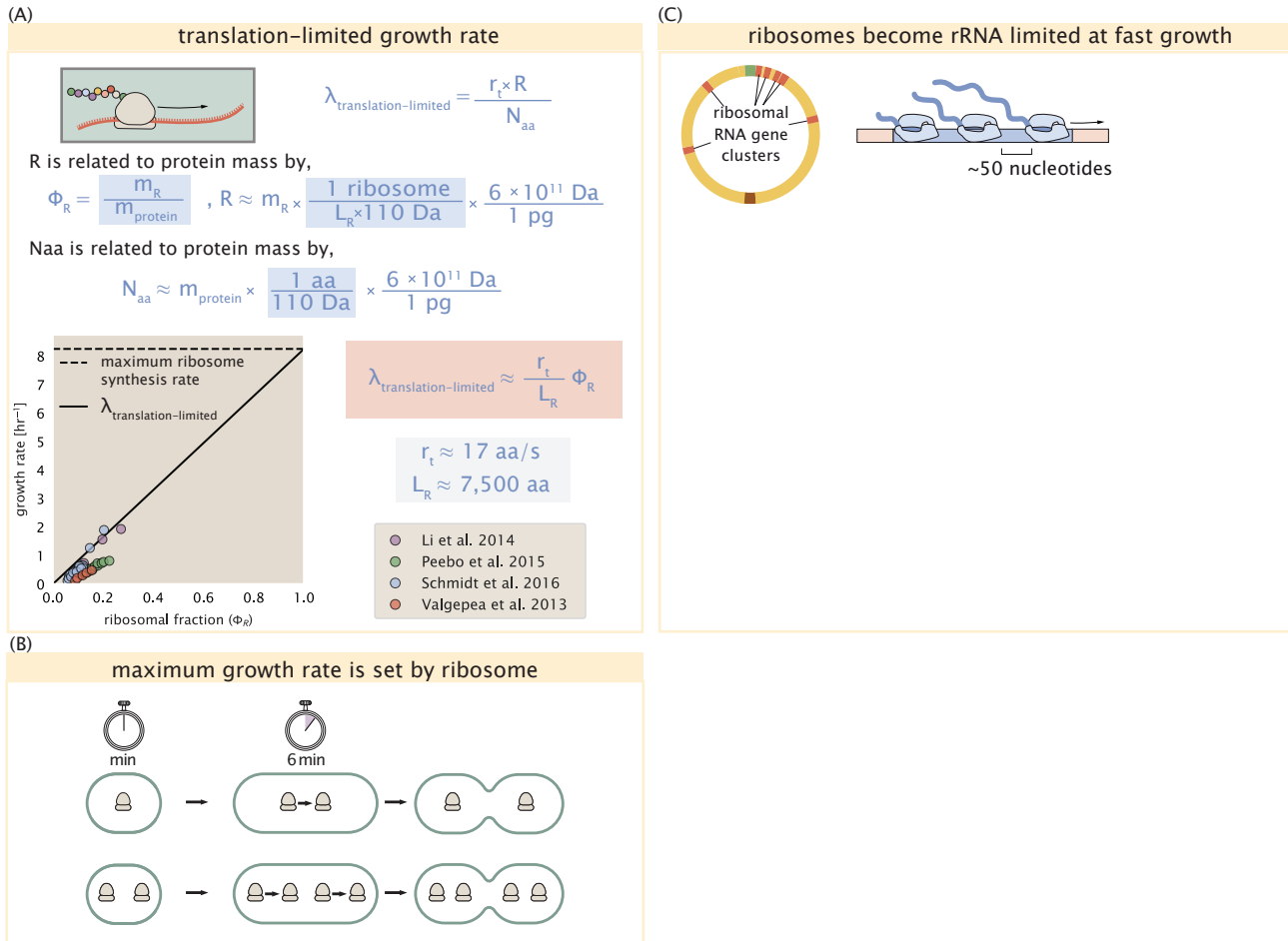


Figure 2. Translation-limited growth rate. (A) Here we consider the translation-limited growth as a function of ribosomal fraction. By mass balance, the time required to double the entire proteome (N_{AA} / r_t) sets the translation-limited growth rate, $\lambda_{\text{translation-limited}}$. Here N_{AA} is effectively the number of peptide bonds that must be translated, r_t is the translation elongation rate, and R is the number of ribosomes. This can also be re-written in terms of the ribosomal mass fraction $\Phi_R = m_R / m_{\text{protein}}$, where m_R is the total ribosomal mass and m_{protein} is the mass of all proteins in the cell. L_R refers to the summed length of the ribosomes in amino acids. $\lambda_{\text{translation-limited}}$ is plotted as a function of Φ_R (solid line). (B) The dashed line in part (A) identifies a maximum growth rate that is set by the ribosome. Specifically, this growth rate corresponds to the time required to translate an entire ribosome, L_R / r_t . This is a result that is independent of the number of ribosomes in the cell as shown schematically here. (C)

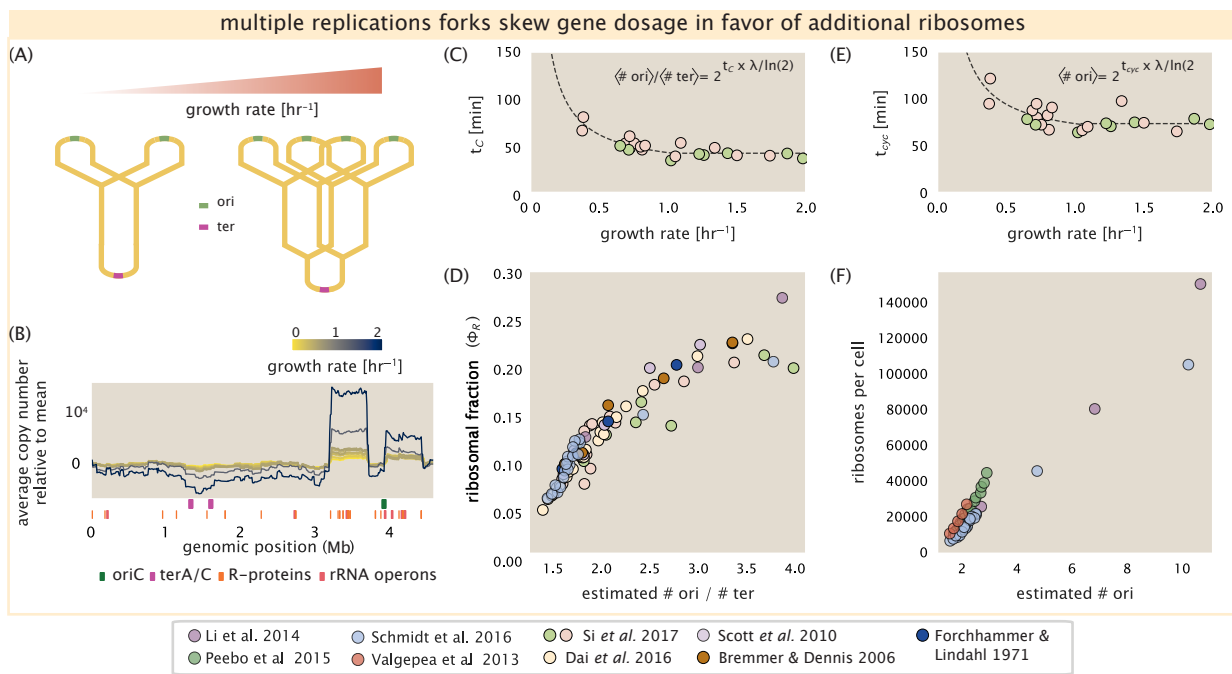


Figure 3. Multiple replication forks skew gene dosage and ribosomal content. (A) Schematic shows the expected increase in replication forks (or number of ori regions) as *E. coli* cells grow faster. (B) A running boxcar average of protein copy number is calculated for each each growth condition considered by Schmidt *et al.*. A 0.5 Mb averaging window was used. Protein copy numbers are reported relative to their condition-specific means in order to center all data sets. (C) and (E) show experimental data from Si *et al.* (2017) Solid lines show fits to the data, which were used to estimate $\langle \# \text{ori} \rangle / \langle \# \text{ter} \rangle$ and $\langle \# \text{ori} \rangle$ [NB: to note fit equations]. Red data points correspond to measurements in strain MG1655, while light green points are for strain NCM3722. (D) Plot compares our estimate of $\langle \# \text{ori} \rangle / \langle \# \text{ter} \rangle$ to the experimental measurements of ribosomal abundance. Ribosomal fraction was approximated from the RNA/protein ratios of Dai *et al.* (2016) (yellow) and Si *et al.* (2017) (light red and light green) by the conversion RNA/protein ratio $\approx \Phi_R \cdot 2.1$. (F) Plot of the ribosome copy number estimated from the proteomic data against the estimated $\langle \# \text{ori} \rangle$.

107 expression under fast growth conditions (dark blue), showing the result. The dramatic change in
 108 protein copy number near the origin is primarily due to the increase in ribosomal protein expression.
 109 This trend is in contrast to slower growth conditions (yellow) where the average copy number is
 110 more uniform across the length of the chromosome.

111 If ribosomal genes (rRNA and ribosomal proteins) are being synthesized at their maximal rate
 112 according to their rRNA gene dosage and maximal transcription rate, we can make two related
 113 hypotheses about how their ribosome abundance should vary with chromosomal content. First,
 114 the ribosomal protein fraction should increase in proportion to the average ratio of DNA origins to
 115 DNA termini ($\langle \# \text{ori} \rangle / \langle \# \text{ter} \rangle$ ratio). This is a consequence of the skew in DNA dosage as cells grow
 116 faster. The second hypothesis is that the absolute number of ribosomes should increase with the
 117 number of DNA origins ($\langle \# \text{ori} \rangle$), since this will reflect the total gene dosage at a particular growth
 118 condition.

119 In order to test each of these expectations we considered the experimental data from Si *et al.*
 120 (2017), which inferred these parameters for cells under nutrient-limited growth. The ratio $\langle \# \text{ori} \rangle /$
 121 $\langle \# \text{ter} \rangle$ depends on how quickly chromosomes are replicated relative the cell's doubling time τ and
 122 is given by $2^{t_c / \tau}$. Here t_c is the time taken to replicate *E. coli*'s chromosome, referred to as the C
 123 period of cell division. In Figure 3(C) we plot the measured t_c versus τ (computed as $\tau = \log(2) / \lambda$),
 124 with data points in red corresponding to *E. coli* strain MG1655, and blue to strain NCM3722. Si *et al.*
 125 (2017) also measured the total RNA to protein ratio which reflects ribosomal abundance and we
 126 show that data along with other recent measurements from Dai *et al.* (2016, 2018). Indeed, we
 127 find that the ribosomal fraction increases with $\langle \# \text{ori} \rangle / \langle \# \text{ter} \rangle$ (Figure 3(C)). We note a systematic
 128 difference in the relative abundances from Peebo *et al.* (2015) and Valgepea *et al.* (2013) that was
 129 inconsistent with a number of other measurements of total RNA-to-protein ratios ($\approx \Phi_R \times 2.1$ Dai

130 *et al. (2016)*) and only show the data from *Schmidt et al. (2016)* and *Li et al. (2014)* for relative
 131 ribosome abundances (see supplemental section XX for a more complete discussion). For the data
 132 shown, the ribosomal fraction doesn't increase as much at higher $\langle \# \text{ ori} \rangle / \langle \# \text{ ter} \rangle$. Since several
 133 rRNA operons are actually located approximately half-way between the origin and terminus, the
 134 trend may in part be a consequence of a diminishing increase in rRNA gene dosage at higher $\langle \# \text{ ori} \rangle / \langle \# \text{ ter} \rangle$ ratios.
 135

136 We can similarly estimate $\langle \# \text{ ori} \rangle$, which depends on how often replication forks are initiated per
 137 cell cycle. This is given by the number of overlapping cell cycles, $2^{\tau_{\text{cyc}}/\tau}$, where τ_{cyc} refers to the total
 138 time of chromosome replication and cell division. *Figure 3(E)* shows the associated data from *Si*
 139 *et al. (2019)*, which we use to estimate $\langle \# \text{ ori} \rangle$ for each growth condition of the proteomic data. In
 140 agreement with our expectations, we find that ribosome copy number increases with the estimated
 141 $\langle \# \text{ ori} \rangle$ (*Figure 3(F)*).
 142

143 While it is difficult to distinguish between causality and correlation, the data is consistent with
 144 the need for cells to increase their effective rRNA gene dosage in order to grow according to the
 145 constraint set by Equation 2. These results may also shed some light on the notable increase in
 146 ribosomal content that is observed when sublethal doses of antibiotics (*Scott et al., 2010; Dai et al.*
 147 *2016*). Specifically, if rRNA synthesis is rate limiting, and nutrient conditions largely dictate the
 148 extent of overlapping DNA replication cycles, than addition of antibiotic will lengthen the doubling
 149 time and allow an increased rRNA synthesis relative to the rate of cell division. In Supplemental
 Section XX, we consider this further using additional data from *Si et al. (2017)*.

150 Regulation of translating ribosomes helps maintain maximal growth according to nutrient
 151 availability.
 152

153 While the above observations show how *E. coli* can vary its ribosomal content to increase growth
 154 rate, it also presents a challenge in the limit of poorer nutrient conditions. Recall from Equation 3
 155 that ribosomal content should decrease to zero as growth decreases to zero. While bacteria tend to
 156 decrease their ribosomal abundance in poorer nutrient conditions, they do so only to some fixed,
 157 non-zero amount (*Scott et al., 2010; Liebermeister et al., 2014*). Here we find a minimal ribosomal
 158 fraction of ≈ 0.06 in the slowest growth conditions. From the perspective of a bacterium dealing
 159 with uncertain nutrient conditions, there is likely a benefit for the cell to maintain some relative
 fraction of ribosomes to support rapid growth as nutrient conditions improve.

160 The challenge however, lies in the cell's ability to maintain growth when ribosomes are in excess
 161 of the rate that nutrients can be harvested and amino acids synthesized for consumption *Figure 4A*.
 162 In the limit of poor growth conditions, ribosomes would consume their amino acid supply and be
 163 unable to maintain steady-state growth. In reality, *E. coli* is still able to maintain a relatively high
 164 elongation rate even in stationary phase ($\approx 8 \text{ AA/s}$, (*Dai et al., 2016, 2018*)). A explanation for this is
 165 that the cell further regulates its biological activity in conditions of stress and nutrient-limitation; in
 166 particular through the small-molecule alarmones (p)ppGpp (*Harris and Theriot, 2018*). In (p)ppGpp
 167 null strains, cells are unable to grow in nutrient-poor media. Indeed, these small molecules play a
 168 role in controlling biosynthesis rates throughout the central dogma [NB citations]. Here we explore
 169 this further in the context of growth by maximizing protein synthesis.

170 We consider slow growth conditions (λ less than 0.5 hr^{-1}) by assuming that the decrease in
 171 elongation rate is due to a limiting supply of amino acids and a need for the cell to maintain excess
 172 nutrients for cellular homeostasis under steady-state growth. There is some experimental support
 173 showing that in poorer nutrient growth conditions, cells have lower amino acids concentrations
 174 (*Bennett et al., 2009*). We proceed by coarse graining the cell's amino acid supply as an single,
 175 effective rate-limiting species (see Supplmental Section XX for a more complete discussion). Under
 176 such a scenario, the elongation rate can described as simply depending on the maximum elongation
 177 rate ($\approx 17.1 \text{ aa/s}$, (*Dai et al., 2016, 2018*)), an effective K_d , and the limiting amino acid concentration

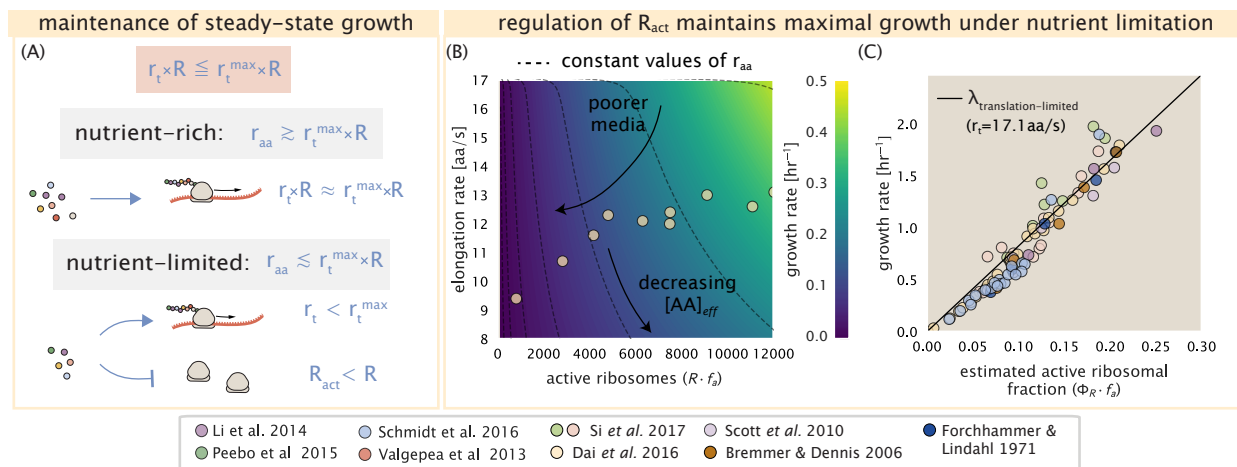


Figure 4. *E. coli* must regulate ribosomal activity in limiting nutrient conditions. (A) Schematic showing translation-specific requirements for maintenance of steady-state growth. In a nutrient rich environment, amino acid supply r_{aa} is sufficiently in excess of the demand by ribosomes translating at their maximal rate. In poorer nutrient conditions, reduced amino acid supply r_{aa} will decrease the rate of elongation. In a regime where r_{aa} is less than $r_t \cdot R$, the number of actively translating ribosomes will need to be reduced in order to maintain steady-state growth. (B) Translation elongation rate is plotted as a function of the number of actively translating ribosomes $R \cdot f_a$. Dashed lines correspond to a range of amino acid synthesis rates r_{aa} , from 10^3 to 10^6 . Growth rates are calculated according to Equation 1, assuming a constant ribosomal fraction of 8 percent. See appendix XX for additional details. (C) Experimental data from Dai *et al.* are used to estimate the fraction of actively translating ribosomes. The solid line represents the translation-limited growth rate for ribosomes elongating at 17.1 AA/s.

178 $[AA]_{eff}$. Specifically, the elongation rate is given by,

$$r_t = r_t^{\max} \cdot \frac{1}{1 + K_d/[AA]_{eff}}. \quad (4)$$

179 For cells growing in minimal media + glucose, the amino acid concentration is of order 100 mM
 180 (BNID: 110093, (Milo *et al.*, 2010; Bennett *et al.*, 2009)). With a growth rate of about 0.6 hr⁻¹ and
 181 elongation rate of 12.5 aa per second (Dai *et al.*, 2016), we can estimate an effective K_d of about 40
 182 mM. Ultimately the steady state amino acid concentration will depend on the difference between
 183 the supply of amino acids r_{aa} and consumption by ribosomes $r_t \cdot R \cdot f_a$, where f_a accounts for the
 184 possible reduction of actively translating ribosomes.

185 In Figure 4B we consider how the maximal growth rate and elongation rates vary as a function
 186 of the number of actively translating ribosomes in this slow growth regime (see Supplemental
 187 Section XX for a complete description of this model). If we consider r_{AA} to be reflective of a specific
 188 growth condition, by considering lines of constant r_{AA} , we find that cells grow fastest by maximizing
 189 their fraction of actively translating ribosomes. When we consider the experimental measurements
 190 from Dai *et al.* (2018), we see that although cells indeed reduce $R \times f_a$, they do so in a way that
 191 keeps $[AA]_{eff}$ relatively constant. Given our estimate for the K_d of 40 mM, we would only expect
 192 a decrease from 100 mM to about 35 mM in the slowest growth conditions. While experimental
 193 data is limited, amino acid concentrations only decrease to about 60 mM for cells grown in minimal
 194 media + acetate ($\lambda = 0.3 \text{ hr}^{-1}$ in our proteomic data; value obtained from Bennett *et al.* (2009)),
 195 qualitatively consistent with our expectations.

196 Given the quantitative data from Dai *et al.* (2018), which determined f_a across the entire range of
 197 growth rates across our data, we next estimated the active fraction of ribosomal protein. As shown
 198 in Figure 4(C), we find that cells grow at a rate near the expected translation maximum expected
 199 from Equation 1, using the maximum elongation rate of $r_t = 17.1 \text{ aa per second}$. This is in contrast
 200 to the reality that ribosomes are translating at almost half this rate in the poorest growth conditions.
 201 This highlights that there are alternative ways to grow according to the translated-limited growth
 202 rate that is expected based with ribosomes translating at their maximal elongation rate. Specifically,
 203 it is by adjusting $r_t \times R \times f_a$ to match maximal growth rate set by Equation 2, through the parameters

204 $r_{tmax} \times R'$, that cells are able to maximize their growth rate under steady-state.

205 Global regulatory control of components of central dogma may provide an explanation
206 for the robust scaling laws in *E. coli*.

207 A number of recent papers further highlight the possibility that (p)ppGpp may even provide a causal
208 explanation for the scaling laws in *E. coli*. In the context of ribosomal activity, increased levels of
209 (p)ppGpp are associated with lower ribosomal content, and at slow growth appear to help reduce the
210 fraction of actively translating ribosomes (*Dai et al., 2016, 2018*). Titration of the cellular (p)ppGpp
211 concentrations (up or down) can invoke similar proteomic changes reminiscent of those observed
212 under nutrient limitation (*Zhu and Dai, 2019*). In light of the limiting dependence of ribosome copy
213 number on chromosomal gene dosage, it was recently shown that growth in a (p)ppGpp null strain
214 abolishes both the scaling in cell size and the $\langle \# \text{ ori} \rangle / \langle \# \text{ ter} \rangle$ ratio. Instead, cells exhibited a high $\langle \#$
215 $\text{ori} \rangle / \langle \# \text{ ter} \rangle$ closer to 4 and cell size more consistent with a fast growth state where (p)ppGpp levels
216 are low (*Fernández-Coll et al., 2020*).]

217 [NB, expand on to consider how activity of RNAP and other aspects(?) may follow a similar
218 behaviour and are under related control mechanisms.]

219 References

- 220 Bennett BD, Kimball EH, Gao M, Osterhout R, Van Dien SJ, Rabinowitz JD. Absolute metabolite concentrations
221 and implied enzyme active site occupancy in *Escherichia coli*. *Nature Chemical Biology*. 2009 Aug; 5(8):593–599.
- 222 Dai X, Zhu M, Warren M, Balakrishnan R, Okano H, Williamson JR, Fredrick K, Hwa T. Slowdown of Translational
223 Elongation in *Escherichia coli* under Hyperosmotic Stress. - PubMed - NCBI. *mBio*. 2018 Feb; 9(1):281.
- 224 Dai X, Zhu M, Warren M, Balakrishnan R, Patsalo V, Okano H, Williamson JR, Fredrick K, Wang YP, Hwa T. Reduction
225 of translating ribosomes enables *Escherichia coli* to maintain elongation rates during slow growth. *Nature Microbiology*. 2016 Dec; 2(2):16231.
- 227 Fernández-Coll L, Maciąg-Dorszynska M, Tailor K, Vadia S, Levin PA, Szalewska-Palasz A, Cashel M, Dunny GM.
228 The Absence of (p)ppGpp Renders Initiation of *Escherichia coli* Chromosomal DNA Synthesis Independent of
229 Growth Rates. *mBio*. 2020 Apr; 11(2):45.
- 230 Godin M, Delgado FF, Son S, Grover WH, Bryan AK, Tzur A, Jorgensen P, Payer K, Grossman AD, Kirschner
231 MW, Manalis SR. Using buoyant mass to measure the growth of single cells. *Nature Methods*. 2010 Apr;
232 7(5):387–390.
- 233 Harris LK, Theriot JA. Surface Area to Volume Ratio: A Natural Variable for Bacterial Morphogenesis. *Trends in
234 microbiology*. 2018 Oct; 26(10):815–832.
- 235 Hui S, Silverman JM, Chen SS, Erickson DW, Basan M, Wang J, Hwa T, Williamson JR. Quantitative proteomic
236 analysis reveals a simple strategy of global resource allocation in bacteria. *Molecular Systems Biology*. 2015
237 Feb; 11(2):e784–e784.
- 238 Li GW, Burkhardt D, Gross C, Weissman JS. Quantifying Absolute Protein Synthesis Rates Reveals Principles
239 Underlying Allocation of Cellular Resources. *Cell*. 2014 Apr; 157(3):624–635. doi: [10.1016/j.cell.2014.02.033](https://doi.org/10.1016/j.cell.2014.02.033).
- 240 Liebermeister W, Noor E, Flamholz A, Davidi D, Bernhardt J, Milo R. Visual account of protein investment in
241 cellular functions. *Proceedings of the National Academy of Sciences*. 2014 Jun; 111(23):8488–8493.
- 242 Maaløe O. Regulation of the Protein-Synthesizing Machinery—Ribosomes, tRNA, Factors, and So On. Goldberger
243 R, editor, *Gene Expression*, Springer; 1979.
- 244 Milo R, Jorgensen P, Moran U, Weber G, Springer M. BioNumbers—the Database of Key Numbers in Molecular
245 and Cell Biology. *Nucleic Acids Research*. 2010 Jan; 38(suppl_1):D750–D753. doi: [10.1093/nar/gkp889](https://doi.org/10.1093/nar/gkp889).
- 246 Peebo K, Valgepea K, Maser A, Nahku R, Adamberg K, Vilu R. Proteome Reallocation in *Escherichia coli* with
247 Increasing Specific Growth Rate. *Molecular BioSystems*. 2015; 11(4):1184–1193. doi: [10.1039/C4MB00721B](https://doi.org/10.1039/C4MB00721B).
- 248 Schaechter M, Maaløe O, Kjeldgaard NO. Dependency on Medium and Temperature of Cell Size and Chemical
249 Composition during Balanced Growth of *Salmonella typhimurium*. *Microbiology*. 1958 Dec; 19(3):592–606.
- 250 Schmidt A, Kochanowski K, Vedelaar S, Ahrné E, Volkmer B, Callipo L, Knoops K, Bauer M, Aebersold R, Heine-
251 mann M. The Quantitative and Condition-Dependent *Escherichia coli* Proteome. *Nature Biotechnology*. 2016
252 Jan; 34(1):104–110. doi: [10.1038/nbt.3418](https://doi.org/10.1038/nbt.3418).
- 253 Scholz SA, Diao R, Wolfe MB, Fivenson EM, Lin XN, Freddolino PL. High-Resolution Mapping of the *Escherichia
254 coli* Chromosome Reveals Positions of High and Low Transcription. *Cell Systems*. 2019 Mar; 8(3):212–225.e9.
- 255 Scott M, Gunderson CW, Mateescu EM, Zhang Z, Hwa T. Interdependence of cell growth and gene expression:
256 origins and consequences. *Science*. 2010 Nov; 330(6007):1099–1102.
- 257 Si F, Le Treut G, Sauls JT, Vadia S, Levin PA, Jun S. Mechanistic Origin of Cell-Size Control and Homeostasis in
258 Bacteria. *Current Biology*. 2019 Jun; 29(11):1760–1770.e7. doi: [10.1016/j.cub.2019.04.062](https://doi.org/10.1016/j.cub.2019.04.062).
- 259 Si F, Li D, Cox SE, Sauls JT, Azizi O, Sou C, Schwartz AB, Erickstad MJ, Jun Y, Li X, Jun S. Invariance of Initiation Mass
260 and Predictability of Cell Size in *Escherichia coli*. *Current Biology*. 2017 May; 27(9):1278–1287.
- 261 Taheri-Araghi S, Bradde S, Sauls JT, Hill NS, Levin PA, Paulsson J, Vergassola M, Jun S. Cell-size control and
262 homeostasis in bacteria. - PubMed - NCBI. *Current Biology*. 2015 Feb; 25(3):385–391.
- 263 Valgepea K, Adamberg K, Seiman A, Vilu R. *Escherichia coli* Achieves Faster Growth by Increasing Catalytic and
264 Translation Rates of Proteins. *Molecular BioSystems*. 2013; 9(9):2344. doi: [10.1039/c3mb70119k](https://doi.org/10.1039/c3mb70119k).
- 265 Zhu M, Dai X. Growth suppression by altered (p)ppGpp levels results from non-optimal resource allocation in
266 *Escherichia coli*. *Nucleic Acids Research*. 2019 Mar; 47(9):4684–4693.